

# bradscholars

## Molecular dynamics and physical stability of amorphous nimesulide drug and its binary drug-polymer systems

Item Type	Article
Authors	Knapik, J.;Wojnarowska, Z.;Grzybowska, K.;Tajber, L.;Mesallati, H.;Paluch, Krzysztof J.;Paluch, M.
Citation	Knapik J, Wojnarowska Z, Grzybowska K, Tajber L, Mesallati H, Paluch KJ and Paluch M (2016) Molecular dynamics and physical stability of amorphous nimesulide drug and its binary drug-polymer systems. Molecular Pharmaceutics. 13(6): 1937–1946.
DOI	<a href="https://doi.org/10.1021/acs.molpharmaceut.6b00115">https://doi.org/10.1021/acs.molpharmaceut.6b00115</a>
Rights	© 2016 ACS. This document is the Accepted Manuscript version of a Published Work that appeared in final form in Molecular Pharmaceutics, copyright © American Chemical Society after peer review and technical editing by the publisher. To access the final edited and published work see <a href="http://dx.doi.org/10.1021/acs.molpharmaceut.6b00115">http://dx.doi.org/10.1021/acs.molpharmaceut.6b00115</a>
Download date	2026-06-08 02:53:22
Link to Item	<a href="http://hdl.handle.net/10454/8380">http://hdl.handle.net/10454/8380</a>

# The University of Bradford Institutional Repository

<http://bradscholars.brad.ac.uk>

This work is made available online in accordance with publisher policies. Please refer to the repository record for this item and our Policy Document available from the repository home page for further information.

To see the final version of this work please visit the publisher's website. Available access to the published online version may require a subscription.

Link to conference webpage: <http://dx.doi.org/10.1021/acs.molpharmaceut.6b00115>

**Citation:** Knapik J, Wojnarowska Z, Grzybowska K, Tajber L, Mesallati H, Paluch KJ and Paluch M (2016) Molecular dynamics and physical stability of amorphous nimesulide drug and its binary drug-polymer systems. *Molecular Pharmaceutics*. 13(6): 1937–1946.

**Copyright statement:** © 2016 ACS. This document is the Accepted Manuscript version of a Published Work that appeared in final form in *Molecular Pharmaceutics*, copyright © American Chemical Society after peer review and technical editing by the publisher. To access the final edited and published work see <http://dx.doi.org/10.1021/acs.molpharmaceut.6b00115>

# Molecular dynamics and physical stability of amorphous nimesulide drug and its binary drug-polymer systems

J. Knapik<sup>1,2\*</sup>, Z. Wojnarowska<sup>1,2</sup>, K. Grzybowska<sup>1,2</sup>, L. Tajber<sup>3</sup>, H. Mesallati<sup>3</sup>, K. J. Paluch<sup>4</sup>, M. Paluch<sup>1,2</sup>

<sup>1</sup>Institute of Physics, University of Silesia, ul. Uniwersytecka 4, 40-007 Katowice, Poland

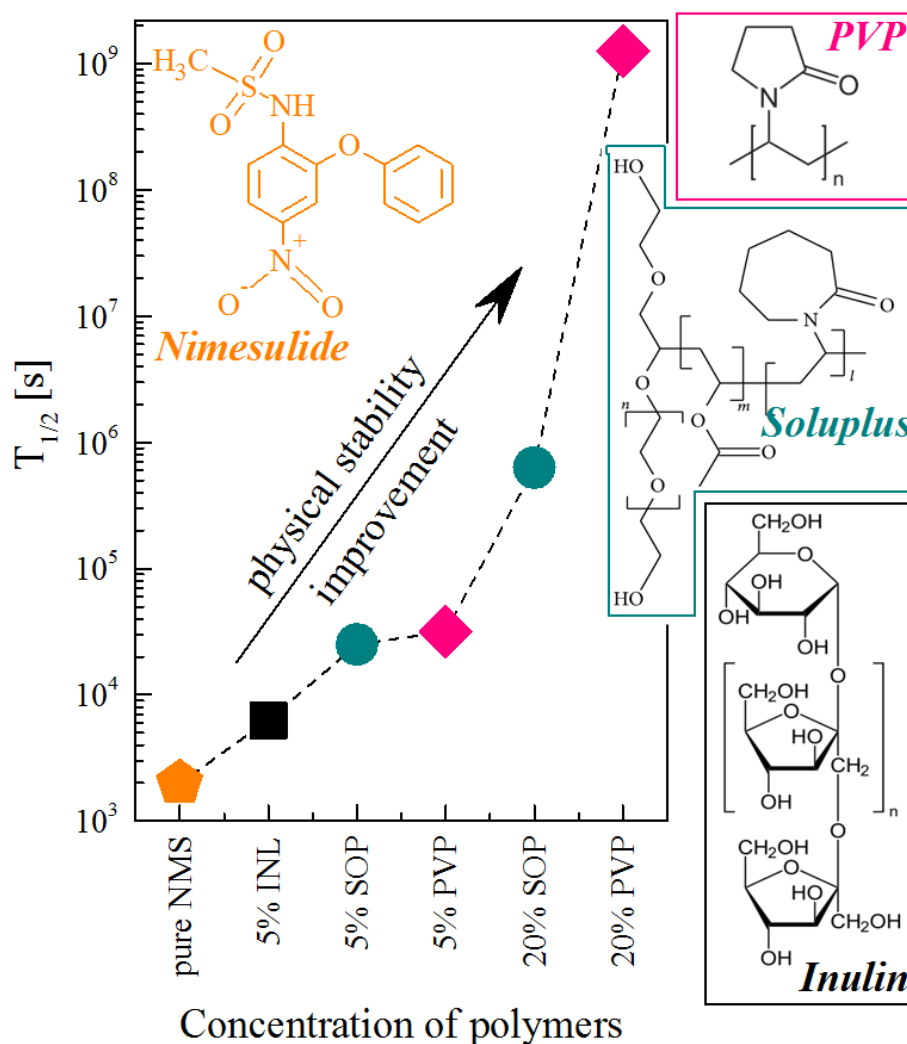
<sup>2</sup>SMCEBI, ul. 75 Pułku Piechoty 1a, 41-500 Chorzów, Poland

<sup>3</sup>School of Pharmacy and Pharmaceutical Sciences, Trinity College Dublin, College Green, Dublin 2, Ireland

<sup>4</sup>Centre for Pharmaceutical Engineering Science, Bradford School of Pharmacy, Faculty of Life Sciences, University of Bradford, Richmond Rd., BD71DP Bradford, W.Yorks., UK.

\*corresponding author: jknapik@us.edu.pl

## Toc



## **ABSTRACT**

In this paper we study the effectiveness of three well known polymers: inulin, Soluplus and PVP in stabilizing amorphous form of nimesulide (NMS) drug. The re-crystallization tendency of pure drug as well as measured drug-polymer systems were examined at isothermal conditions by using broadband dielectric spectroscopy (BDS), and at non-isothermal conditions by differential scanning calorimetry (DSC). Our investigation has shown that the crystallization half-life time of pure NMS at 328 K is equal to 33 minutes. We found that this time can be prolonged to 40 years after adding to NMS 20% of PVP polymer. This polymer proved to be the best NMS's stabilizer, while the worst stabilization effect was found after adding the inulin to NMS. Additionally, our DSC, BDS and FTIR studies indicate that for suppression of NMS's re-crystallization in NMS-PVP system, the two mechanisms are responsible: the polymeric steric hindrances as well as the antiplastization effect exerted by the excipient.

## **KEY WORDS**

amorphous drug, physical stability, molecular dynamics, nimesulid, drug-polymer system, PVP, Soluplus, inulin

## INTRODUCTION

Nimesulid (NMS) is a non-steroidal anti-inflammatory drug (NSAIDs) which shows high anti-inflammatory, antipyretic, and analgesic activities in addition to low toxicity, and a high therapeutic index<sup>1</sup>. Like many non-steroidal anti-inflammatory drugs, NMS is characterized by low aqueous solubility ( $\approx 0.01$  mg/mL), and poor dissolution rate<sup>2</sup>. The commonly employed strategies to increase solubility and dissolution rate of poorly soluble drugs are based on using an cyclodextrin, macronization, and conversion the Active Pharmaceutical Ingredients (APIs) to their salt forms<sup>3</sup>. Another, an alternative way is preparing the amorphous form of those compounds. Recently, it has been often reported that pharmaceuticals prepared in the amorphous form are significantly more soluble, have higher dissolution rate, and have greater bioavailability than their crystalline counterparts<sup>4,5,6</sup>. Unfortunately, it should be highlighted that, amorphous APIs are in general physically unstable and, consequently, during storage or manufacturing they may revert to the crystalline form and, consequently, lose their superior properties.<sup>7,8,9,10</sup>

It is believed that the main factor affecting physical stability of disordered APIs is molecular mobility<sup>11,12</sup>. It has been demonstrated many times that the most efficient experimental tool to investigate molecular dynamics of glass-forming systems is broadband dielectric spectroscopy (BDS)<sup>13,14</sup>. This technique enables the determination of the characteristic time of molecular reorientation over a broad range of frequencies (over 12 decades) and temperatures. Such a wide  $f$  and  $T$  range allows the detection of various relaxation processes. In the supercooled liquid, the structural ( $\alpha$ ) relaxation, which originates from cooperative movements of many molecules, is usually the most prominent relaxation process observed in the dielectric spectra. In the glassy state it is possible to observe faster local motions, which have an inter- or intramolecular origin. Additionally, using dielectric spectroscopy, the kinetics of crystallization at isothermal conditions can be monitored. Such studies are extremely valuable, especially for physical stability tests.

The objective of the current work was to convert nimesulid drug to its amorphous form and examine by means of BDS its physical stability. Since, our measurements indicate that amorphous NMS is extremely physically unstable system, a lot of attention has been paid to find an efficient method of stabilization this material. A promising strategy for inhibiting devitrification of amorphous drugs is to disperse them into a polymeric matrix.<sup>15,16,17</sup> Therefore we decided to check how three well known and commonly used in pharmaceutical industry polymers: inulin (INL), Soluplus (SOP) and poly(vinylpyrrolidone) (PVP) stabilize nimesulid drug. It is worth noting that each of these additives belong to different groups of

polymers. SOP represents a very complex copolymeric system, whereas both INL and PVP have strictly one polymerizable unit. In contrast to inulin, which has a stiff molecular chain, poly(vinylpyrrolidone) belongs to a group of polymers with highly flexible structures. In order to achieve our aim and answer the question of which polymer can better suppress NMS's crystallization, we investigated the molecular dynamics and kinetics of crystallization of pure NMS and the following binary mixtures: NMS+PVP, NMS+SOP and NMS+INL. The crystallization process in nimesulide has been examined at both isothermal and non-isothermal conditions. The latter was measured by using differential scanning calorimetry (DSC). Finally, we also tried to establish which stabilization mechanism is involved in case of the investigated binary mixtures.

## EXPERIMENTAL METHODS

### *Materials*

Nimesulide (NMS) (Kemprotec Limited, UK), inulin DP-23 (INL) (Frutafix TEX, Sensus, Netherlands), polyvinyl pyrrolidone 10 kDa (PVP) (Sigma Aldrich, Ireland) and Soluplus<sup>TM</sup> (SOP) (BASF, Germany).

### *Preparation of physical mixtures*

Physical mixtures of NMS and polymers, respectively; INL, PVP or SOP were prepared by milling at room temperature using mixer mill MM 200 (Retsch, Germany) for 15 min at mixing frequency of 25 1/s.

### *Differential Scanning Calorimetry (DSC)*

Thermodynamic properties of NMS, NMS + 5% wt. INL, NMS + 5% wt. SOP, NMS + 5% wt. PVP, NMS + 20% wt. SOP and NMS + 20% wt. PVP were examined using a Mettler–Toledo DSC 1 STAR<sup>e</sup> System. The measuring device was equipped with HSS8 ceramic sensor having 120 thermocouples and liquid nitrogen cooling station. The instrument was calibrated for temperature and enthalpy using zinc and indium standards. Crystallization and melting points were determined as the onset of the peak, whereas the glass transition temperature as the midpoint of the heat capacity increment. The samples were measured in an aluminum crucible (40  $\mu$ L). All measurements were carried out in range from 270 K to 430/435 K with a variety – 5 K/min, 10 K/min, 20 K/min and 30 K/min – of heating rates.

### *Broadband Dielectric Spectroscopy (BDS)*

Dielectric measurements of NMS, NMS + 5% wt. INL, NMS + 5% wt. SOP, NMS + 5% wt. PVP, NMS + 20% wt. SOP and NMS + 20% wt. PVP were carried out using a Novo-Control GMBH Alpha dielectric spectrometer, in the frequency range from  $10^{-1}$  Hz to  $10^6$  Hz, at temperatures from 193 K to 328 K with steps of 2.5 K. The temperature was controlled by a Quattro temperature controller with temperature stability better than 0.1 K. Dielectric studies of all samples were performed immediately after fast cooling of the melt in a parallel-plate cell made of stainless steel (diameter 15 mm and a 0.1 mm gap with Teflon spacers). Crystallization kinetics for all samples were carried out at four different temperatures, as follows: pure NMS at 318 K, 323 K, 328 K and 330.5 K; NMS + 5% INL at 318 K, 323 K, 328 K and 333 K; NMS + 5% SOP at 328 K, 330.5 K, 333 K and 338 K; NMS + 5% PVP

at 328 K, 330.5 K, 333 K and 338 K; NMS + 20% SOP at 343 K, 353 K, 358 K and 363 K; NMS + 20% PVP at 360.5 K, 363 K, 365.5 K and 368 K.

*Fourier Transform Infrared Spectroscopy (FTIR)*

FTIR was performed using a Spectrum One FT-IR Spectrometer (Perkin Elmer, Connecticut, USA) equipped with Spectrum Software version 6.1. A spectral range of 450-4000  $\text{cm}^{-1}$ , resolution of 4  $\text{cm}^{-1}$ , scan number of 10 and scan speed of 0.2  $\text{cm/s}$  were used. KBr disks were produced by direct compression, using a pressure of approximately 10 bar for 1 minute. A sample loading of 1% was used. The spectra were normalized and background corrected.

## MOLECULAR DYNAMICS OF PURE NIMESULIDE ABOVE AND BELOW THE GLASS TRANSITION

Dielectric loss spectra of amorphous nimesulide were measured in both the supercooled liquid and glassy state by using BDS technique. In this experiment, the temperature was increased from 193 K to 328 K in steps of 2.5 K. Representative spectra are shown in Figure 1. For better visualization of obtained dielectric results, the data have been divided into two panels (a and b). Panel a of Figure 1 presents spectra collected above the glass transition temperature. Herein, we can see one well-resolved loss peak connected to the  $\alpha$ -relaxation process. This relaxation mode moves toward higher frequencies with increasing temperature and at  $T > 323$  K its intensity begins to rapidly decrease. Such a drop in the intensity of  $\alpha$ -relaxation is caused by cold crystallization of the sample and it reflects the degree of reduction in amorphous fraction.<sup>18</sup> In order to determine the value of  $\beta_{KWW}$  for NMS, and to check whether temperature affects the shape of the structural relaxation process, we constructed so-called masterplot (see inset Figure 1a) by horizontal shifting of spectra (taken at different temperatures from 300.65 to 323.15 K) to superimpose on the reference spectrum at 303.15 K. As can be seen in presented masterplot, the shape of the structural relaxation in NMS is not changing with temperature, and the parameter  $\beta_{KWW}$  is the same for all spectra and equal to 0.72. According to the Shamblin observations, narrower  $\alpha$ -relaxation peaks correspond to higher physical stability of amorphous APIs.<sup>19</sup> However, as our studies show, the amorphous NMS reveals quite a strong tendency to recrystallize, despite of fact that the  $\alpha$ -relaxation peak is quite narrow. Similar behavior was previously observed in the case of ezetimibe, celecoxib and sildenafil.<sup>20,21,22,23</sup>

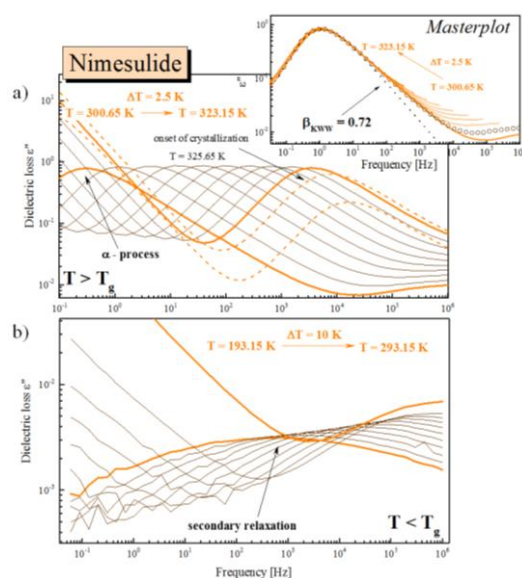


**Figure 1.** Dielectric loss spectra of NMS obtained on heating. The panel (a) presents spectra collected above the glass transition temperature, whereas panel (b) shows spectra below the  $T_g$ . In the inset of panel (a) we present the masterplot that was constructed by superimposed dielectric spectra at nine different temperatures above  $T_g$ . The dashed black line represents the KWW fit with the  $\beta_{KWW} = 0.72$ .

Panel b of Figure 1 presents dielectric spectra collected at temperatures below  $T_g$ . In this temperature region the structural relaxation becomes too slow to be observed and only secondary relaxation processes may be visible. As can be easily seen in Figure 1b, NMS has only one secondary ( $\beta$ ) process, which, just like the  $\alpha$ -mode, moves toward higher frequencies with increasing temperature. However, this process is less sensitive to temperature changes when compared to the behavior of the  $\alpha$ -relaxation.

From analysis of dielectric loss spectra collected above and below  $T_g$ , we determined the temperature dependence of  $\alpha$ - and  $\beta$ -relaxation times (see Figure 2). Firstly, to obtain the values of  $\tau_\alpha$  and  $\tau_\beta$  at various temperatures, the asymmetric  $\alpha$ -peak and symmetric  $\beta$ -process have been fitted using the Havriliak–Negami (HN) and the Cole–Cole (CC) function, respectively.<sup>24</sup> The empirical HN approach is given by the formula:

$$\varepsilon_{HN}^*(\omega) = \varepsilon'(\omega) - i\varepsilon''(\omega) = \varepsilon_\infty + \frac{\Delta\varepsilon}{[1 + (i\omega\tau_{HN})^a]^b} \quad (1)$$

where  $\varepsilon'$  and  $\varepsilon''$  are real and imaginary parts of complex dielectric permittivity,  $\varepsilon_\infty$  is high frequency limit permittivity,  $\Delta\varepsilon$  is dielectric strength,  $\tau_{HN}$  is the HN relaxation time, and  $a$  and  $b$  represent symmetric and asymmetric broadening of the relaxation peak. This function is equivalent to the CC function when the parameter  $b$  is equal to 1. In this special case Eq. (1) fits NMS's  $\beta$ -relaxation.<sup>25</sup> Next, the fitting parameters were used to calculate the  $\tau_\alpha$  and  $\tau_\beta$  by means of the equation:

$$\tau_{\alpha/\beta} = \tau_{HN} \left[ \sin\left(\frac{\pi a}{2 + 2b}\right) \right]^{-1/a} \left[ \sin\left(\frac{\pi ab}{2 + 2b}\right) \right]^{1/a} \quad (2)$$

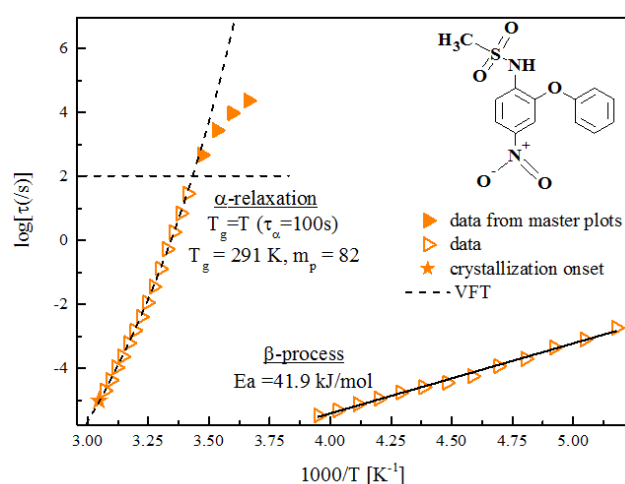


**Figure 2.** The relaxation map of NMS drug. Temperature dependence of  $\tau_\alpha$  in the supercooled liquid has been described by the VFT equation. The  $\alpha$ -relaxation times in the glassy state were found by horizontal shift of the structural relaxation peak from the region above the glass transition to the region below  $T_g$ . The temperature dependence of  $\tau_\beta$  was fitted using the Arrhenius equation.

In order to parameterize the  $\tau_\alpha(T)$  dependence we employed the Vogel–Fulcher–Tammann (VFT) equation:

$$\tau_\alpha(T) = \tau_\infty \exp\left(\frac{B}{T - T_0}\right) \quad (3)$$

where  $\tau_\infty$ ,  $T_0$ , and  $B$  are fitting parameters.<sup>26,27,28</sup> Their values for NMS are equal to:  $\log_{10}(\tau_\infty/s) = -19.4 \pm 0.7$ ,  $T_0 = 216 \pm 4$ , and  $B = 3711 \pm 310$ . Based on the VFT parameters we estimated  $T_g$  (defined as  $\tau_\alpha = 100$  s) of NMS as 291 K. The glass transition temperature determined by this method is in good agreement with the  $T_g$  obtained from calorimetric studies ( $T_{gDSC\ 10K/min} = 294$  K – see Figure 5) as well as with the literature data.<sup>29</sup> From VFT fits we also calculated the value of the fragility parameter for NMS as  $m_p = 82$ . This parameter, also called steepness index, is a measure of deviation from Arrhenius behavior of the  $\tau_\alpha(T)$  dependence and is defined as follows:<sup>30</sup>

$$m_p = \left. \frac{d \log \tau_\alpha}{d(T_g/T)} \right|_{T=T_g} \quad (4)$$

Typical values of steepness index are between 16 and 200. The higher the value of  $m_p$ , the more fragile (less strong) liquids are. The fragility is frequently considered as a key parameter for researchers dealing with physical stability of amorphous drugs because it has been implied that strong materials are more stable than fragile ones.<sup>31</sup> However, very recently a few exceptions to this correlation were found. In the case of NMS we found that its low physical stability correlates to a high value of fragility. Thus NMS satisfies the above mentioned correlation.

#### **ISOTHERMAL AND NON-ISOTHERMAL CRYSTALLIZATION KINETICS STUDIES OF PURE NMS ABOVE THE GLASS TRANSITION TEMPERATURE**

In this section we shall concentrate on the crystallization kinetics of NMS drug. To fully characterize the tendency of amorphous NMS to devitrify, both the isothermal and non-isothermal kinetics of crystallization have been investigated.

The isothermal cold crystallization kinetics of NMS were studied by using BDS technique. In this experiment, we performed time-depending dielectric measurements at four different temperatures (318 K, 323 K, 328 K and 330.5 K). For each measurement a new sample was prepared by employing the vitrification method. Using dielectric spectroscopy the crystallization process can be followed by measuring both the real ( $\epsilon'$ ) and imaginary ( $\epsilon''$ ) parts of the complex dielectric permittivity. In the  $\epsilon'$ , devitrification is reflected by a decrease

in the static permittivity (Figure 3a), whereas in the  $\epsilon''$  by a decrease in the intensity of the  $\alpha$ -loss peak (Figure 3b).

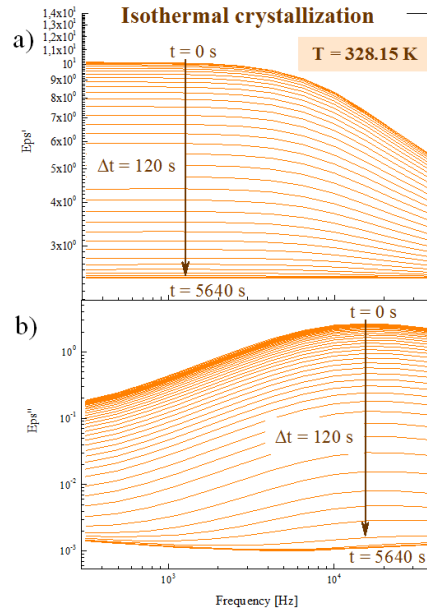


**Figure 3. Dielectric spectra of the real (a) and imaginary (b) parts of the complex dielectric permittivity during an isothermal cold crystallization of NMS at fixed temperature equal to 238 K.**

Usually, the progress of cold crystallization is analyzed by normalized dielectric constant ( $\epsilon'_N$ ), defined as follows:

$$\epsilon'_N(t) = \frac{\epsilon'(0) - \epsilon'(t)}{\epsilon'(0) - \epsilon'(\infty)} \quad (5)$$

where  $\epsilon'(0)$  is the dielectric constant at the beginning of the crystallization process,  $\epsilon'(t)$  is the value of dielectric constant at time  $t$ , and  $\epsilon'(\infty)$  is the long-time limiting value. The normalized kinetics curves of NMS are presented together in Figure 4.

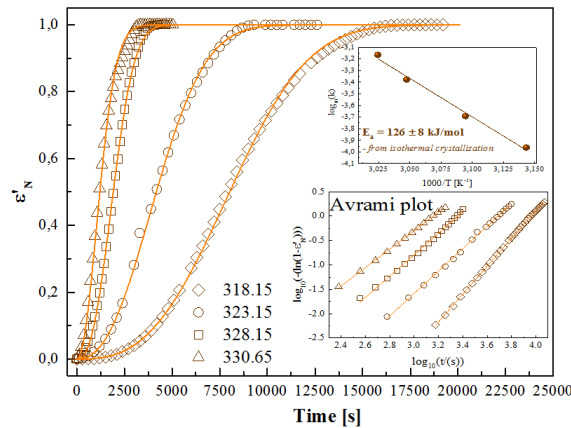


**Figure 4. Normalized dielectric constant  $\epsilon'_N$  as a function of time from crystallization processes occurring at: 318.15, 323.15, 328.15 and 330.65 K. The lower inset presents the Avrami plots in terms of eq. 6 for each crystallization temperature in the time ranges where the dependences are linear. The upper inset shows the temperature dependence of  $\log k$  – here, the solid line denotes the linear fit of eq. 7.**

To analyze the time dependence of  $\varepsilon'_N$  we used the Avrami model.<sup>32</sup> It should be mentioned that this model is the most commonly applied method of analyzing the crystallization process at a fixed temperature, and is described by the following formula:

$$\varepsilon'_N(t) = 1 - \exp(-K(t)^n) \quad (6)$$

where  $K=k^n$  is the rate constant, and  $n$  is the Avrami parameter that is directly related to the nucleation dimensionality. Usually parameter  $n$  falls in the range of 2-3.<sup>33</sup> To determine values of both  $K$  and  $n$  parameters we prepared a so-called Avrami plot (see lower inset of Figure 4), which is based on the equation:<sup>34</sup>

$$\log(-\ln(1 - \varepsilon'_N(t))) = \log K(t) + n \log t \quad (7)$$

As can be clearly seen, if the  $\log(-\ln(1 - \varepsilon'_N(t)))$  vs.  $\log t$  is linear, the  $n$  and  $\log K$  can be determined as the slope and the intercept of this dependence, respectively. Avrami parameters obtained in this way are shown in Table 1. The value of Avrami exponent  $n$  changes in the standard way, i.e. decreases with temperature (from 2.9 to 1.8), indicating that the crystallization process of NMS at isothermal conditions is three- and two-dimensional at high and low temperatures, respectively. Additionally, since the parameter  $K$  increases with increasing crystallization temperature, we can conclude that the dominant mechanism of isothermal devitrification in the case of NMS is the diffusion of molecules.<sup>35</sup>

T [K]	n	logK
318.15	2.86 ± 0.01	- 11.33 ± 0.04
323.15	2.30 ± 0.02	- 8.49 ± 0.07
328.15	2.18 ± 0.03	- 7.36 ± 0.10
330.65	1.89 ± 0.01	- 5.98 ± 0.03

**Table 1. Isothermal cold crystallization kinetics parameters of NMS obtained from the Avrami model according to eq. 7.**

In order to estimate the activation energy of isothermal cold crystallization ( $E_{al}$ ) for NMS we plotted the logarithm of  $k$  ( $k=K^{1/n}$ ) versus reciprocal temperature (see upper inset of Figure 4). Since the  $\log k$  vs.  $1000/T$  dependence, in measured temperature range, is linear, the value of  $E_{al}$  may be found by fitting Arrhenius law to the experimental points:

$$\log k = \log k_0 - \frac{E_{al}}{RT} \log e \quad (8)$$

where  $k_0$  and  $E_{al}$  are fitting parameters, and  $R$  is the universal gas constant. It should be pointed out the temperature dependence of crystallization might not be linear if the measured temperature range would be wider. Crystallization activation energy of pure NMS obtained in this way is equal to  $126 \pm 8$  kJ/mol.

The cold crystallization kinetics of NMS was also studied at non-isothermal conditions. For these measurements the DSC technique was employed. During the experiment the sample was heated from 270 K to 430 K at different heating rates  $\phi = 5, 10, 20$  and  $30$  K/min. As can be seen in Figure 5 and Table 2, with increasing heating rate the values of  $T_g$ ,  $T_o$  (temperature of crystallization onset) and  $T_p$  (temperature of crystallization peak) shift toward higher temperatures.

Heating Rate [K/min]	$T_o$ [K]	$T_p$ [K]	$T_g$ [K]
5	342	348	293
10	348	354	294
20	352	360	296
30	359	365	298

**Table 2.** Temperatures of crystallization onsets, peaks and glass transitions determined from DSC thermograms measured at different heating rates.

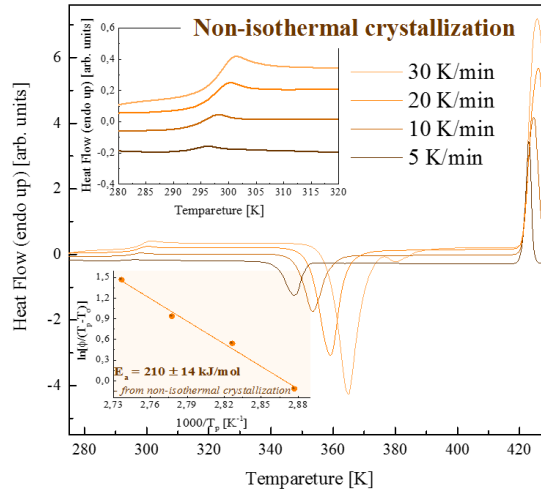


**Figure 5.** DSC thermograms of NMS measured at different heating rates (5 K/min, 10 K/min, 20 K/min, 30 K/min). The upper inset shows an enlarged temperature region of the glass transitions. The lower inset presents an Augiss and Bennett plot for the crystallization peak of NMS. The orange line indicates the linear fit to eq. 9.

Based on the parameters collected in Table 2, we determined the activation energy of non-isothermal cold crystallization ( $E_{aNI}$ ) of NMS by using the Augiss and Bennett approach (see lower inset of Figure 5):<sup>36</sup>

$$\ln\left(\frac{\phi}{T_p - T_o}\right) = C_{AB} - \frac{E_{aNI}}{RT_p} \quad (9)$$

where  $C_{AB}$  and  $E_{aNI}$  are fitting parameters and  $R$  is the universal gas constant. The activation energy obtained using this method is significantly greater (over 35%) than the crystallization activation energy of NMS at isothermal conditions, and is equal to  $210 \pm 14$  kJ/mol.

Further analysis of non-isothermal cold crystallization kinetics of NMS was carried out based on the temperature dependence of relative degree of crystallinity  $X$ .<sup>37</sup> The  $X(T)$

dependence, for each heating rate, is presented in Figure 6a, and was obtained by using the following equation:

$$X(T) = \frac{\int_{T_0}^T (dH_c/dT)dT}{\int_{T_0}^{T_\infty} (dH_c/dT)dT} \quad (10)$$

where  $T_0$  and  $T_\infty$  represent the temperatures at which the crystallization process begins and ends, respectively, while  $dH_c$  denotes the enthalpy of crystallization that is released during an infinitesimal temperature range  $dT$ .

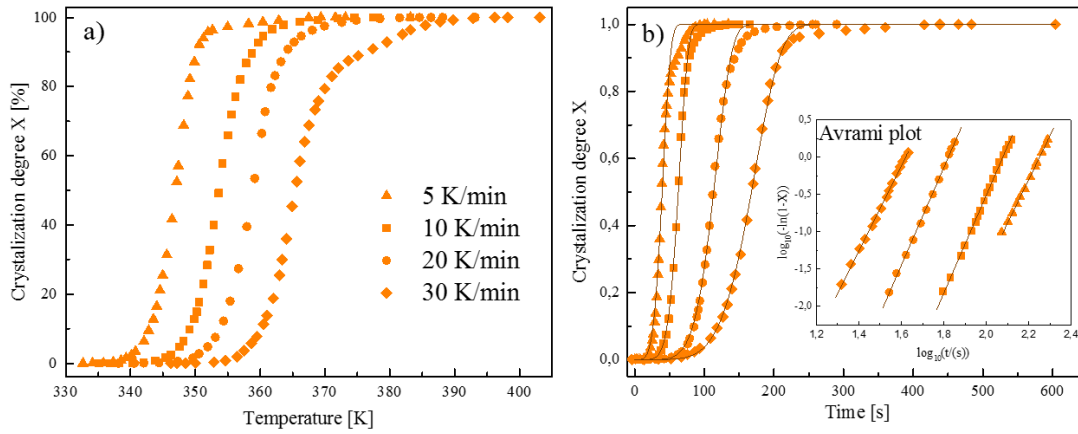


**Figure 6. (a) The temperature dependence of crystallization degree determined from eq. 10 at different heating rates. (b) The time dependence of crystallization degree obtained by transforming the temperature scale into the time scale using eq. 11. The inset presents the Avrami plots, which have been constructed from the non-isothermal crystallization data for NMS.**

After determination of the  $X(T)$  dependence it was possible to transform the temperature scale into the time scale and consequently obtain  $X(t)$  function. For this transformation the equation listed below has been used:

$$t = \frac{T - T_0}{\phi} \quad (11)$$

where  $t$  denotes the time of crystallization and  $\phi$  is the heating rate. The plots of the relative degree of crystallinity as a function of time at different heating rates are shown in Figure 6b.  $X(t)$  dependence was next analyzed by the Avrami model – inset of Figure 6b. Obtained values of  $n'$  and  $\log K'$  are shown in Table 3.

$\phi$ [K/min]	$n'$	$\log K'$
5	$5.86 \pm 0.05$	$-13.20 \pm 0.11$
10	$6.78 \pm 0.05$	$-14.07 \pm 0.11$
20	$6.52 \pm 0.08$	$-11.89 \pm 0.14$
30	$5.57 \pm 0.07$	$-9.04 \pm 0.11$

**Table 3. Non-isothermal cold crystallization kinetics parameters of NMS obtained from the Ozawa model according to eq. 11.**

As can be seen, the  $n'$  parameter changes from 5.6-6.8, indicating that the non-isothermal cold crystallization of NMS is much more complicated than crystallization at fixed temperature, where parameter  $n$  oscillated around 2.5. This is probably due to the formation of more than one crystallographic structure at non-isothermal conditions. The formation of various polymorphs also might explain higher  $E_a$  of crystallization at non-isothermal conditions than at fixed temperature.

#### **THE EFFECTS OF POLYMERIC ADDITIVES ON PHYSICAL STABILITY OF AMORPHOUS NMS**

In this part of the paper we shall investigate how three polymers that are frequently used in the pharmaceutical industry, Soluplus (SOP), inulin (INL) and poly(vinylpyrrolidone) (PVP), affect the physical stability of the amorphous form of NMS. Since one of the main factors affecting the re-crystallization of disordered pharmaceuticals is molecular mobility, the NMS + polymer systems have been investigated by means of BDS technique. The dielectric loss spectra of systems containing NMS drug and the polymeric additive were measured at the temperature range from 173.15 K to 338.15 K with step of 2.5 K. The representative spectra of the binary amorphous mixtures with 5% of the polymers are presented in Figure 7. As can be seen, all three mixtures exhibit one well resolved secondary relaxation process below the glass transition temperature (lower panels of Figure 7 a, b and c). All these processes are similar to that found in pure NMS, and therefore it is concluded that they originate from dipole reorientation of the drug's molecules. Above the  $T_g$  a well pronounced relaxation peak, corresponding to the structural  $\alpha$ -relaxation process, is observed in the dielectric spectra (see upper panels of Figure 7 a, b and c). It moves toward higher frequencies with increasing temperature, and its intensity begins to rapidly decrease at  $T = 326$  K for NMS + 5% INL, and  $T = 343$  K – for NMS + 5% SOP and NMS + 5% PVP. This drop in intensity of the  $\alpha$ -peak is due to the crystallization onset.

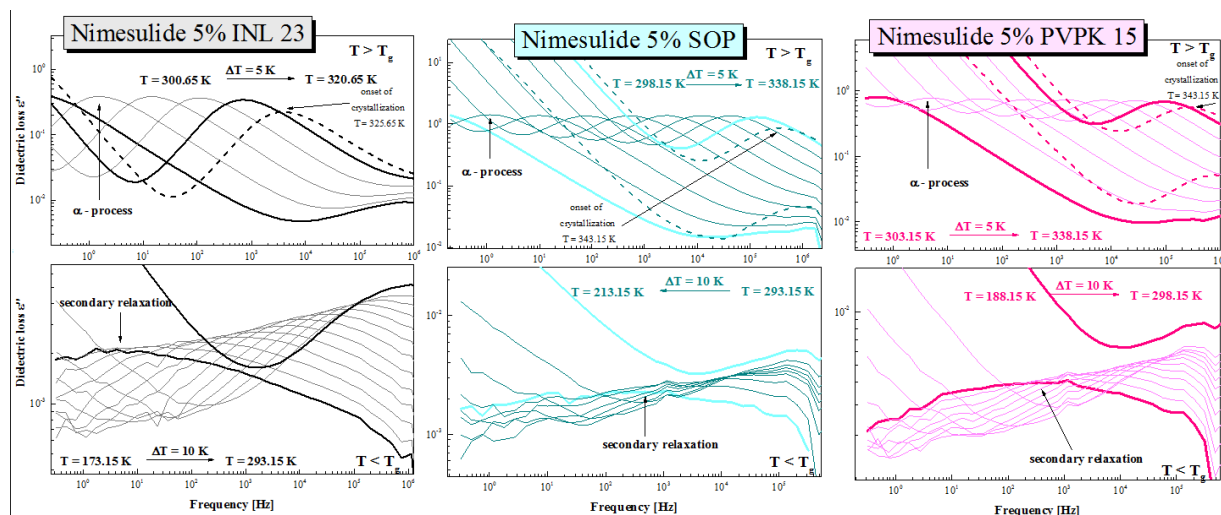


**Figure 7.** Dielectric loss spectra of binary amorphous mixtures of NMS drug and 5% weight of INL (black panels), SOP (cyan panels) and PVP (pink panels) obtained on heating. The upper panels present spectra collected above the glass transition temperature, whereas lower panels show spectra below the  $T_g$ .

As can be seen, the devitrification of the mixture containing 5% of INL begins at lower temperature than for the other mixtures. Therefore we can conclude that INL stabilizes NMS the least. Similar result has been obtained by using DSC experiment (see Figure 8). The heating rate applied in these DSC experiments is equal to 10 K/min.

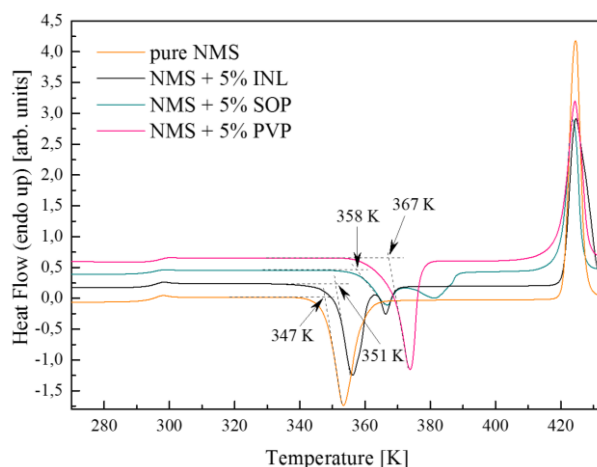


**Figure 8.** The DSC thermograms of pure NMS, NMS + 5% of INL, NMS + 5% of SOP, and 5% of PVP measured at heating rates equal to 10 K/min.

In order to check how higher concentration of PVP and SOP will affect on NMS's physical stability, we additionally prepared for further studies the mixtures of NMS + SOP and, NMS + PVP with a higher (20% weight) concentration of the polymers. From the analysis of dielectric loss spectra collected both above and below the  $T_g$  of all examined systems (i.e. NMS + 5% INL, NMS + 5% SOP, NMS + 5% PVP, NMS + 20% SOP and NMS + 20% PVP), the temperature dependences of  $\alpha$ - and  $\beta$ - relaxation times for all of these mixtures (see Figure 9) were obtained. To determine the  $\tau_\alpha$  and  $\tau_\beta$  we employed the same method used previously for pure NMS.

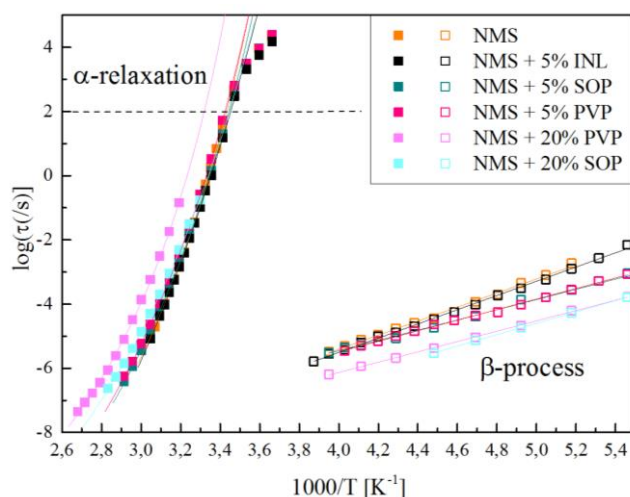


**Figure 9.** Relaxation maps of NMS and mixtures containing NMS and 5% or 20% polymer (INL,SOP or PVP). Temperature dependence of  $\tau_\alpha$  in the supercooled liquid has been described by VFT equation. The temperature dependence of  $\tau_\beta$  was fitted by using the Arrhenius equation.

The Vogel-Fulcher-Tamman equation was used to describe the  $\tau_\alpha(T)$  dependences, while the  $\tau_\beta(T)$  dependences were fitted to the Arrhenius law. The fitting parameters for the VFT and the Arrhenius equations are collected in Table 4. As can be seen in Figure 9 the greatest changes in the temperature dependence of structural relaxation times can be observed in the case of the mixtures containing PVP, suggesting that this polymer may be the most successful at stabilizing the amorphous form of NMS drug.

Sample	$\alpha$ -process			$\beta$ -process	
	$T_0$ [K]	$\log \tau_{\alpha-a}$	B	$\log \tau_{\alpha-\beta}$	$E_\beta$ [kJ/mol]
Pure NMS	$216.1 \pm 3.8$	$-19.4 \pm 0.7$	$3711 \pm 310$	$-14.2 \pm 0.2$	$41.9 \pm 0.9$
NMS + 5% INL	$182.4 \pm 5.4$	$-24.8 \pm 1.0$	$6609 \pm 568$	$-14.4 \pm 0.1$	$42.4 \pm 0.5$
NMS + 5% SOP	$210.9 \pm 3.9$	$-19.2 \pm 0.6$	$3881 \pm 299$	$-11.8 \pm 0.2$	$30.4 \pm 0.7$
NMS + 5% PVP	$213.0 \pm 2.2$	$-19.1 \pm 0.4$	$3841 \pm 171$	$-12.1 \pm 0.1$	$31.5 \pm 0.5$
NMS + 20% SOP	$198.1 \pm 6.6$	$-19.3 \pm 0.8$	$4499 \pm 485$	$-13.4 \pm 0.1$	$33.9 \pm 0.4$
NMS + 20% PVP	$237.9 \pm 4.8$	$-15.7 \pm 0.6$	$2588 \pm 259$	$-12.6 \pm 0.1$	$30.8 \pm 0.3$

**Table 4.** The fitting parameters from the VFT and Arrhenius equations.

In order to check how effectively the stability of disordered NMS was improved by using the examined polymers, the isothermal kinetics of crystallization, at four various temperatures for NMS's mixtures containing 5% INL, 5% SOP, 5% PVP, 20% SOP and 20% PVP, have been measured. Since the tested mixtures exhibit different tendencies to crystallize, it was not always possible to measure them at the same temperatures. The crystallization kinetics studies were carried out at 318 K, 323 K, 328 K and 333 K for NMS + 5% INL; at 328 K, 330.5 K, 333 K and 338 K for NMS + 5% SOP; at 328 K, 330.5 K, 333 K and 338 K for NMS + 5% PVP, at 343 K, 353 K, 358 K and 363 K for NMS + 20% SOP; and at 360.5 K, 363 K, 365.5 K and 368 K for NMS + 20% PVP. For each measurement a new sample was prepared by the vitrification method.

The method used to analyze the crystallization kinetics of all samples was analogous to that used for pure NMS, i.e. using the Avrami model. The temperature dependences of the logarithm of the crystallization rate  $k$  are presented in Figure 10. This plot has the fundamental purpose of answering the following two questions: i) how do the polymeric additives change the crystallization activation energy?; and ii) what is the difference in the  $\log k$  values of pure NMS and various binary amorphous mixtures at fixed temperature?

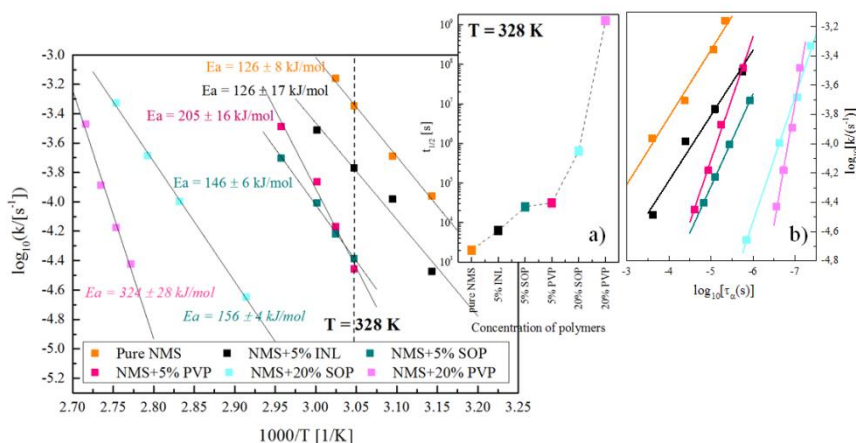


**Figure 10.** The temperature dependence of  $\log(k)$  of pure NMS and binary amorphous mixtures containing the drug and 5% or 20% polymer (INL, SOP or PVP). Solid lines in this figure denote the linear fit to the Arrhenius equation. The inset a presents the crystallization half-life time of NMS and all prepared mixtures checked at a temperature of 328 K. The inset b present the  $\log_{10}k$  as a function of  $\log_{10}t_{1/2}$ .

The crystallization activation energy of the mixture containing 5% INL is comparable to the value of 126 kJ/mol estimated for the pure NMS. In contrast, both 5% additive of SOP and 5% additive of PVP result in an increase in this value. The  $E_a$  of NMS + 5% SOP and NMS + 5% PVP are equal to  $146 \pm 6 \text{ kJ/mol}$  and  $205 \pm 16 \text{ kJ/mol}$ , respectively. A greater amount of SOP polymer (20%) brings about an increase in the activation energy of crystallization to  $156 \pm 4 \text{ kJ/mol}$ . However, the most significant effect has been observed after adding 20% PVP to NMS. In this case, the activation energy reached the highest value of  $324 \pm 28 \text{ kJ/mol}$ .

A useful measure of the capability of polymers to stabilize the NMS drug is the crystallization half-life time ( $t_{1/2}$ ).<sup>38</sup> It defines the time required to reach half of the final crystallinity and it has been calculated for each measured sample at  $T = 328 \text{ K}$  by using the following relation:

$$t_{1/2} = \left( \frac{\ln 2}{K} \right)^{1/n} \quad (12)$$

The values of  $t_{1/2}$  are plotted versus concentration of polymers in the inset of Figure 10. As can be seen, the half-life time at  $T = 328 \text{ K}$  for pure NMS is equal to 33 min, while for samples

containing 5% INL, SOP and PVP  $t_{1/2} = 1.8$  h,  $t_{1/2} = 6.7$  h and  $t_{1/2} = 8.8$  h, respectively. If the concentration of SOP and PVP is raised to 20% the values of  $t_{1/2}$  are equal to 7.3 days for SOP and 40 years for PVP.

The results presented above indicate that INL has indeed the least stabilizing effect on the examined drug from all tested polymers, while the highest inhibition of crystallization was observed with mixtures containing PVP – the polymer which has the greatest impact on NMS's molecular mobility.

In order to find out if the suppression of the drug's re-crystallization in NMS-PVP mixtures is caused only by the antiplastization effect, we examined how the glass transition temperatures of NMS-PVP mixtures change with the polymer concentration. It has been demonstrated many times that if additional interactions between the drug and polymer exist, the experimentally determined  $T_g$  values for different concentrations of the additive should deviate from the theoretical dependence that was proposed by Gordon and Taylor:<sup>39,40</sup>

$$T_g = \frac{w_1 T_{g1} + K w_2 T_{g2}}{w_1 + K w_2} \quad (13)$$

where  $w_1$  and  $w_2$  are the weight fractions of each component, and  $T_{g1}$  and  $T_{g2}$  correspond to the glass transition temperature of each component.  $T_g$  is the glass transition temperature of the mixture, while  $K$  is a measure of the interaction between the components, and can be defined as follows:<sup>41</sup>

$$K \approx \frac{\Delta C_{p2}}{\Delta C_{p1}} \quad (14)$$

where  $\Delta C_p$  denotes the change in heat capacity at  $T_g$ .

It can be clearly seen in Figure 11 that the  $T_g$  values of the NMS-PVP mixture grow continuously with increasing polymer content. A noticeable discrepancy between the predicted values of glass transition temperature and the experimentally determined data was observed. Therefore one can expect that, apart from an antiplasticizing effect also the specific interactions between the drug and excipient, and/or polymeric steric hindrances, may also play an important role in improving NMS's physical stability in binary amorphous NMS-PVP systems.

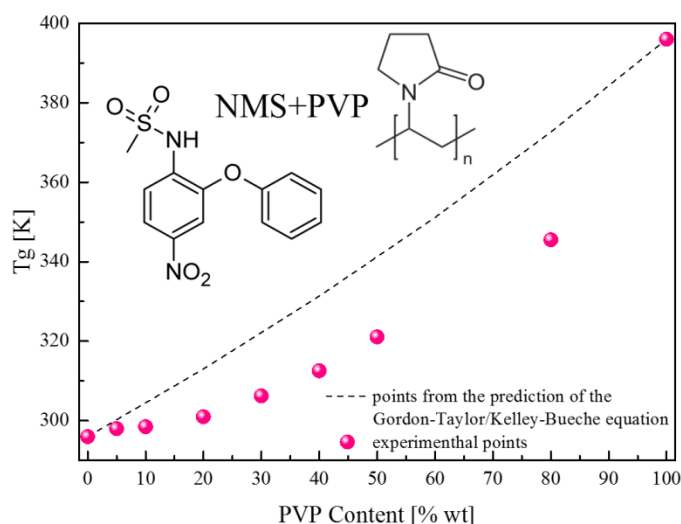


**Figure 11.** Glass transition temperatures of the NMS–PVP mixtures. The pink circles correspond to the experimentally determined  $T_g$  values, whereas the dashed line represents the prediction of the Gordon–Taylor/Kelley–Bueche equation, calculated from the  $T_g$  values of the pure NMS and pure PVP K15. In the inset the chemical structures of both compounds are presented.

To check if specific chemical interactions indeed exist in NMS-PVP mixtures, we performed a series of FTIR experiments. Table 5 presents the position of the main absorption peaks (band assignment was carried out based on work of Galico et al.<sup>42</sup> and Tajber et al.<sup>43</sup>) and Figure 11 shows selected FTIR spectra of the amorphous samples. It can be seen that, with exception of the CO stretching vibration of PVP, the bands remained practically at the same position, regardless of the sample composition. The  $\nu_{\text{CO}}$  band showed, however, a blue shift as the NMS content in the sample increased, which indicates that this chemical group becomes less H-bonded in the presence of the drug, most likely due to the more hydrophobic environment limiting the moisture content. Overall, FTIR analysis indicates that NMS and PVP did not interact in the amorphous phase and the overall net of H-bond interactions decreased, consistent with large negative deviations of the  $T_g$  values from the prediction, as presented in Figure 11. Consequently, the suppression of NMS’s crystallization in NMS-PVP mixtures should be caused by two mechanisms: the polymeric steric hindrances as well as the antiplastization effect exerted by the additive.

NMS (% w/w)	NMS						PVP	
	$\nu_{\text{NH}}$	$\nu_{\text{CC}_{\text{ring}}}$	$\nu_{\text{aNO}_2}$	$\rho_{\text{rNH}} + \rho_{\text{rCH}_{\text{ring}}} + \nu_{\text{aSO}_2}$	$\nu_{\text{CN}_{\text{nitro}}} + \nu_{\text{sNO}_2}$	$\nu_{\text{sSO}_2}$	$\nu_{\text{CO}}$	$\nu_{\text{CN}}$
<b>100</b>	3284	1599,1589	1522	1343	1318	1154	N/A	N/A
<b>95</b>	3284	1599,1589	1522	1343	1318	1155	1678	N/A
<b>90</b>	3285	1599,1588	1521	1343	1317	1154	1680	N/A

<b>80</b>	N/A	1598,1588	1524	1341	N/A	1156	1676	N/A
<b>60</b>	N/A	1597,1587	1523	1341	N/A	1157	1676	N/A
<b>40</b>	N/A	1596,1587	1523	1341	N/A	1157	1673	1289
<b>20</b>	N/A	1597,1587	1523	1340	N/A	1156	1670	1289
<b>10</b>	N/A	N/A	1524	1339	N/A	1157	1665	1290
<b>0</b>	N/A	N/A	N/A	N/A	N/A	N/A	1664	1290

**Table 5.** Position of principal FTIR bands of amorphous NMS, PVP and NMS-PVP mixtures (N/A – not applicable;  $\nu$  – stretching,  $\nu_a$  – asymmetric stretching,  $\nu_s$  – symmetric stretching, and  $\rho_r$  – rocking vibration).

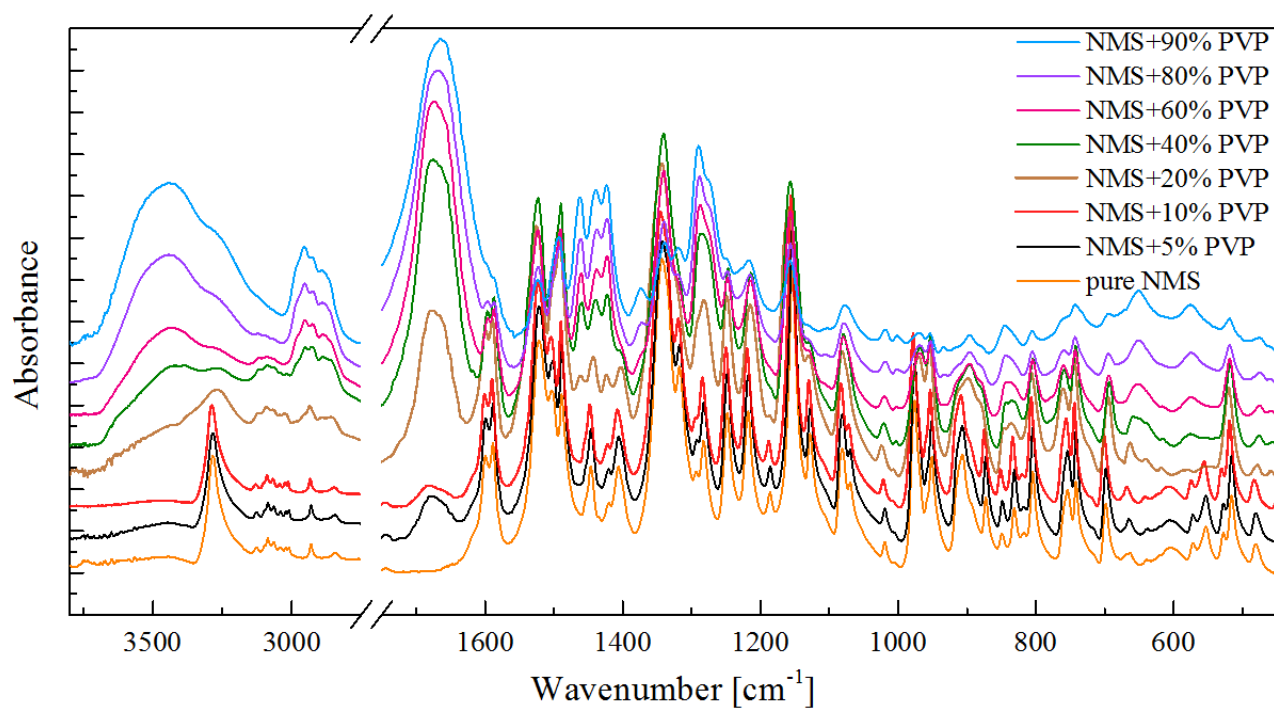


**Figure 12.** FTIR spectra of amorphous NMS-PVP systems

## CONCLUSIONS

In this paper we investigated how three well known polymers, inulin, Soluplus and PVP, affect the physical stability and molecular mobility of amorphous nimesulide drug. Using broadband dielectric spectroscopy the molecular mobility of pure drug and mixtures containing 5% or 20% wt. of the polymers has been completely characterized. Besides the  $\alpha$ -relaxation, NMS and binary amorphous mixtures exhibit one secondary mode. Both the BDS and DSC studies have shown that pure drug easily re-crystallized. To get a full picture of the tendency of amorphous NMS to devitrify, we measured isothermal and non-isothermal kinetics of crystallization. Based on the data we calculated the isothermal and non-isothermal crystallization activation energies. Their values are equal to  $126 \pm 8$  kJ/mol and  $210 \pm 14$  kJ/mol, respectively. The significantly greater (over 35%) value of  $E_{aNI}$  than  $E_{aI}$  can result from the formation of polymorphs during NMS's crystallization. We also found that the dominant mechanism of devitrification in the case of NMS drug is the diffusion of molecules.

In order to experimentally investigate the effectiveness of crystallization inhibition of the drug by polymeric additives we measured the isothermal crystallization kinetics of all tested substances. Based on these studies we calculated the crystallization activation energies as well as the crystallization half-life times at 328 K of all measured substances. The  $E_a$  and  $t_{1/2}$ (at 328 K) of pure NMS, NMS + 5% INL, NMS + 5% SOP, NMS + 5% PVP, NMS + 20% SOP, and NMS + 20% PVP are equal to  $126 \pm 8$  kJ/mol and 33 min,  $126 \pm 14$  kJ/mol and 1.8 h,  $146 \pm 6$  kJ/mol and 6.7 h,  $205 \pm 16$  kJ/mol and 8.8 h,  $156 \pm 4$  kJ/mol and 7.3 days, and  $324 \pm 28$  kJ/mol and 40 years, respectively.

Our studies indicate that INL is the worst stabilizer for NMS, whereas the most significant stabilization effect can be achieved by adding the polymer PVP to NMS. Probably, the two mechanisms are responsible for suppression of NMS's re-crystallization in NMS-PVP system: the polymeric steric hindrances, and the antiplastization effect exerted by the excipient.

## ACKNOWLEDGMENTS

The authors J.K., Z.W., K.G. and M.P., are grateful for the financial support received within the Project No. 2015/16/W/NZ7/00404 (SYMFONIA 3) from the National Science Centre, Poland. H.M. and L.T. are supported by Science Foundation Ireland under grant No. 12/RC/2275 (Synthesis and Solid State Pharmaceuticals Centre).

- 
- <sup>1</sup> Davis N, Brogden RN – (1994) Nimesulide: an update of its pharmacodynamic and pharmacokinetic properties and its therapeutic efficacy, *Drugs*, 48(3):431–454.
- <sup>2</sup> Purcaru S.O., Ionescu M., Raneti C., Anuta V., Mircioiu I., Belu I., Study of Nimesulide Release from Solid Pharmaceutical Formulations in Tween 80 Solutions. *Current Health Sciences Journal* 2010, 36(1), 42-47.
- <sup>3</sup> Adrjanowicz K., Wojnarowska Z., Wlodarczyk P., Kaminski K., Paluch M., J. Mazgalski, Molecular mobility in liquid and glassy states of Telmisartan (TEL) studied by Broadband Dielectric Spectroscopy. *European Journal of Pharmaceutical Sciences* 2009, 38, 395–404.
- <sup>4</sup> Lipinski, C., 2002. Poor aqueous solubility—an industry wide problem in drug delivery. *Am. Pharm. Rev.* 5, 82–85.
- <sup>5</sup> Rasenack, N., Müller, B.W., 2005. Poorly water-soluble drugs for oral delivery: a challenge for pharmaceutical development. Part I: Physicochemical and biopharmaceutical background/strategies in pharmaceutical development. *Pharmazeutische Industrie* 67 (3), 323–326.
- <sup>6</sup> Kaminski, K.; Adrjanowicz, K.; Wojnarowska, Z.; Grzybowska, K.; Hawelek, L.; Paluch, M.; Zakowiecki, D.; Mazgalski, J. Molecular dynamics of the cryomilled base and hydrochloride ziprasidones by means of dielectric spectroscopy. *J. Pharm. Sci.* 2011, 2642–2657.
- <sup>7</sup> Yoshioka, M., Hancock, B.C., Zografi, G., 1994. Crystallization of indomethacin from the amorphous state below and above its glass transition temperature. *J. Pharm. Sci.* 83, 1700.
- <sup>8</sup> Bhugra, C., Pikal, M., 2007. Role of thermodynamic, molecular, and kinetic factor in crystallization from amorphous state. *J. Pharm. Sci.* 97, 1329–1349.
- <sup>9</sup> Knapik, J., Wojnarowska, Z., Grzybowska, K., Jurkiewicz, K., Tajber, L., Paluch, M., Molecular Dynamics and Physical Stability of Coamorphous Ezetimib and Indapamide Mixtures. *Mol. Pharmaceutics* 2015, 12 (10),3610-3619.
- <sup>10</sup> Bhardwaj, S. P.; Suryanarayanan, R. Molecular mobility as an effective predictor of the physical stability of amorphous trehalose. *Mol. Pharmaceutics* 2012, 9 (11), 3209–3217.
- <sup>11</sup> Adrjanowicz, K.; Kaminski, K.; Paluch, M.; Wlodarczyk, P.; Grzybowska, K.; Wojnarowska, Z.; Hawelek, L.; Sawicki, W.; Lepek, P.; Lunio, R. Dielectric relaxation studies and dissolution behavior of amorphous verapamil hydrochloride. *J. Pharm. Sci.* 2010, 99, 828–839.

- 
- <sup>12</sup> Kothari, K., Ragoonanan, V.; Suryanarayanan, R. The Role of Drug–Polymer Hydrogen Bonding Interactions on the Molecular Mobility and Physical Stability of Nifedipine Solid Dispersions. *Mol. Pharmaceutics* 2015, 12, 162–170
- <sup>13</sup> Johari G.P., Kim S., Shanker R.M., Dielectric study of equimolar acetaminophen-aspirin, acetaminophen-quinidine, and benzoic acid-progesterone molecular alloys in the glass and ultraviscous states and their relevance to solubility and stability. *J Pharm Sci.* 2010, 99(3), 1358-74.
- <sup>14</sup> Bhardwaj S. P. , Arora K. K., Kwong E., Templeton A., Clas S.D., Suryanarayanan R., Mechanism of Amorphous Itraconazole Stabilization in Polymer Solid Dispersions: Role of Molecular Mobility. *Mol. Pharmaceutics* 2014, 11(11), 4228–4237.
- <sup>15</sup> Laitinena, R.; Lobmanna, K.; Strachana, C. J.; Grohganzb, H.; Radesa, T. Emerging trends in the stabilization of amorphous drugs. *International Journal of Pharmaceutics* 453 (2013) 65– 79
- <sup>16</sup> Eerdenbrugh, B.; Taylor, L. S. Small Scale Screening To Determine the Ability of Different Polymers To Inhibit Drug Crystallization upon Rapid Solvent Evaporation. 7(4) (2010) 1328–1337
- <sup>17</sup> Taylor, T. S.; Zografi, G. Spectroscopic Characterization of Interactions Between PVP and Indomethacin in Amorphous Molecular Dispersions. 14(12) (1997) 1691–1698
- <sup>18</sup> Adrjanowicz, K.; Grzybowski, A.; Grzybowska, K.; Pionteck, J.; Paluch, M. Toward Better Understanding Crystallization of Supercooled Liquids under Compression: Isochronal Crystallization Kinetics Approach. *Cryst. Growth Des.* 2013, 13, 4648–4654
- <sup>19</sup> Shamblin, S. L.; Tang, X.; Chang, L.; Hancock, B. C.; Pikal, M. J. Characterization of the time scales of molecular motion in pharmaceutically important glasses. *J. Phys. Chem. B* 1999, 103, 4113–4121.
- <sup>20</sup> Knapik, J.; Wojnarowska, Z.; Grzybowska, K.; Hawelek, L.; Sawicki, W.; Wlodarski, K.; Markowski, J.; Paluch, M. Physical Stability of the Amorphous Anticholesterol Agent (Ezetimibe): The Role of Molecular Mobility. *Mol. Pharmaceutics* 2014, 11, 4280–4290.
- <sup>21</sup> Grzybowska, K.; Paluch, M.; Wlodarczyk, P.; Grzybowski, A.; Kaminski, K.; Hawelek, L.; Zakowiecki, D.; Kasprzycka, A.; Jankowska-Sumara, I. Enhancement of amorphous celecoxib stability by mixing it with octaacetylmaltose: the molecular dynamics study. *Mol. Pharmaceutics* 2012, 9 (4), 894–904.
- <sup>22</sup> Grzybowska, K.; Paluch, M.; Wlodarczyk, P.; Grzybowski, A.; Kaminski, K.; Hawelek, L.; Zakowiecki, D.; Kasprzycka, A.; Jankowska-Sumara, I. Enhancement of amorphous

---

celecoxib stability by mixing it with octaacetylmaltose: the molecular dynamics study. *Mol. Pharmaceutics* 2012, 9 (4), 894–904.

<sup>23</sup> Kolodziejczyk, K.; Paluch, M.; Grzybowska, K.; Grzybowski, A.; Wojnarowska, Z.; Hawelek, L.; Ziolo, J. D. Relaxation Dynamics and Crystallization Study of Sildenafil in the Liquid and Glassy States. *Mol. Pharmaceutics* 2013, 10 (6), 2270–2282.

<sup>24</sup> Kremer, F., Schön hals, A., Eds. *Broadband Dielectric Spectroscopy*; Springer: Berlin, 2003.

<sup>25</sup> Schönhals, A.; Kremer, F. Analysis of Dielectric Spectra. In *Broadband Dielectric Spectroscopy*; Kremer, F., Schön hals, A., Eds.; Springer Verlag: Berlin, 2003; Chapter 3.

<sup>26</sup> Vogel, H. Das Temperaturabhängigkeitgesetz der Viskosität von Flüssigkeiten. *J. Phys. Z.* 1921, 22, 645–646.

<sup>27</sup> Fulcher, G. S. Analysis of Recent Measurements of the Viscosity of Glasses. *J. Am. Ceram. Soc.* 1925, 8, 339–355.

<sup>28</sup> Tammann, G.; Hesse, W. Die Abhängigkeit der Viskosität von der Temperatur bei unterkühlten Flüssigkeiten. *Z. Anorg. Allg. Chem.* 1926, 156, 245–257.

<sup>29</sup> Trasi, N. S.; Baird, J. A.; Kestur, U. S.; Taylor L. S. Factors Influencing Crystal Growth Rates from Undercooled Liquids of Pharmaceutical Compounds. *J. Phys. Chem.* 2014, 118 (33), 9974–9982.

<sup>30</sup> Bohmer, R.; Ngai, K. L.; Angell, C. A.; Plazek, D. J. Nonexponential relaxations in strong and fragile glass formers. *J. Chem. Phys.* 1993, 99, 4201.

<sup>31</sup> Wojnarowska, Z.; Grzybowska, K.; Hawelek, L.; Dulski, M.; Wrzalik, R.; Gruszka, I.; Paluch, M.; Pienkowska, K.; Sawicki, W.; Bujak, P.; Paluch, K. J.; Tajber, L.; Markowski, J.; Molecular Dynamics, Physical Stability and Solubility Advantage from Amorphous Indapamide Drug. *Mol. Pharm.*, 2013, 10(10), 3612–3627.

<sup>32</sup> Avrami, M. Kinetics of Phase Change. I General Theory. *J. Chem. Phys.* 1939, 7, 1103.

<sup>33</sup> Kaminski, K.; Adrjanowicz, K.; Wojnarowska, Z.; Paluch, M.; Kaminska, E.; Kasprzycka, A. Do intermolecular interactions control crystallization abilities of glass forming liquids? *J. Phys. Chem. B* 2011, 115 (40), 11537–11547

<sup>34</sup> Xue, M.-L.; Sheng, J.; Yu, Y.-L.; Chuah, H. H. Nonisothermal crystallization kinetics and spherulite morphology of poly(trimethylene terephthalate). *European Polymer Journal* 40 (2004) 811–818.

- 
- <sup>35</sup> Massalska-Arodz, M.; Williams, G.; Smith, I. K.; Conolly, C.; Aldridge, G. A.; Dabrowski, R. Molecular dynamics and crystallization behaviour of isopentyl cyanobiphenyl as studied by dielectric relaxation spectroscopy. *J. Chem. Soc., Faraday Trans.* 1998, 94, 387–394.
- <sup>36</sup> Augis, J. A.; Bennett, J. E. Calculation of the Avrami parameters for heterogeneous solid state reactions using a modified the Kissinger method. *J. Therm. Anal.* 1978, 13, 283–292.
- <sup>37</sup> Wang, Y.; Shen, C.; Chen, J. Nonisothermal Cold Crystallization Kinetics of Poly(ethylene terephthalate)/Clay Nanocomposite. *Polymer Journal*, 2003, 35(11), 884—889.
- <sup>38</sup> Wu, H.; Qiu Z. Synthesis, crystallization kinetics and morphology of novel poly(ethylene succinate-co-ethylene adipate) copolymers. *Cryst. Eng. Comm.*, 2012, 14, 3586-3595.
- <sup>39</sup> Gordon, M.; Taylor, J. S. Ideal copolymers and the 2nd-order transitions of synthetic rubbers 1. Non-crystalline copolymers. *J. Appl. Chem.* 1952, 2, 493–500.
- <sup>40</sup> Kelley, F. N.; Bueche, F. Viscosity and glass temperature relations for polymer diluent systems. *J. Polym. Sci.* 1961, 50, 549–556.
- <sup>41</sup> Couchman, P. R.; Karasz, F. E. A classical thermodynamic discussion on the effect of composition on glass-transition temperatures. *Macromolecules* 1978, 11, 117–119.
- <sup>42</sup> Gálico, D. A.; Perpétuo, G. L.; Castro, R. A. E.; Treu-Filho, O.; Legendre, A. O.; Galhiane, M. S.; Bannach G. Thermoanalytical study of nimesulide and their recrystallization products obtained from solutions of several alcohols. *J. Therm. Anal. Calorim.* 2014, 115 (3), 2385-2390.
- <sup>43</sup> Tajber, L.; Corrigan, O. I.; Healy, A. M. Physicochemical evaluation of PVP-thiazide diuretic interactions in co-spray-dried composites--analysis of glass transition composition relationships. *Eur J Pharm Sci.* 2005, 24(5), 553-563.